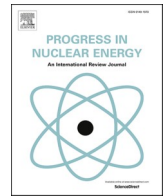




Contents lists available at ScienceDirect

## Progress in Nuclear Energy

journal homepage: <http://www.elsevier.com/locate/pnucene>

# Feasibility study on application of an artificial neural network for automatic design of a reactor core at the Kyoto University Critical Assembly

Song Hyun Kim<sup>a,\*</sup>, Sung Gyun Shin<sup>a</sup>, Sangsoo Han<sup>a</sup>, Moo Hwan Kim<sup>a</sup>, Cheol Ho Pyeon<sup>b</sup>

<sup>a</sup> Division of Advanced Nuclear Engineering, Pohang University of Science and Technology, Pohang, 37673, Republic of Korea

<sup>b</sup> Nuclear Engineering Science Division, Research Reactor Institute, Kyoto University, Asashiro-nishi, Kumatori-cho, Sennan-gun, Osaka, 590-0494, Japan

## ARTICLE INFO

## Keywords:

KUCA  
Artificial neural network  
Reactor core design  
Research reactor  
Optimization

## ABSTRACT

Designing reactor cores by means of an artificial neural network is a difficult challenge, because there are many variables in the core configuration. Especially, for designing a new type of reactor core with an artificial neural network, little (if any) previous data exists, and the appropriate number of results, such as multiplication factors and neutron fluxes, which require a large computational time for a single calculation, should be previously obtained for training the machine learning of the artificial neural network. This paper presents a feasibility study on the automatic design of a research reactor core (a simplified core based on the Kyoto University Critical Assembly) using an artificial neural network. By imitating conventional design procedure, a way to design the core is developed by means of the artificial neural network and automatic machine learning. After setting a design goal of the reactor core, the fuel assembly and core are designed by the proposed method and compared with those designed by conventional design procedure. The results reveal that the reactor core designed by the proposed method performs well and will, therefore, provide a clue to innovation in future reactor design with artificial intelligence.

## 1. Introduction

The Kyoto University Critical Assembly (KUCA) is a research reactor used to investigate reactor characteristics, especially for newly developed reactors. The core configurations at KUCA can be flexibly changed for individual experimental purposes: Statics or kinetics experiments for investigation of the accelerator-driven system were performed (Persson et al., 2008; Pyeon et al., 2009; Kim et al., 2017a, 2017b; Kim et al., 2018a, 2018b); specific core configurations were pursued, such as a <sup>232</sup>Th-loaded reactor and a Solid Pb–Bi experiment (Yamanaka et al., 2016; Pyeon et al., 2016). In the researches and experiments, the core configurations have been designed, manually. However, to obtain an optimized design for each experimental purpose, much human resources and time have been required. Also, core configurations designed by the conventional procedure cannot guarantee high performances for individual experimental purpose.

Recently, artificial intelligence (AI) has been applied to many engineering fields, including electronics, unmanned vehicles, mobile phones, medical diagnosis, and robotics. One of the notable changes in AI techniques is the application of the deep-learning system (Yann

LeCun et al., 2015). Especially, reinforcement learning and unsupervised learning can carry out machine learning without previous big data and can effectively train the artificial neural network. Therefore, AI can conduct semi-creative works, such as design optimizations (Nozaki et al., 2017; Poteralski and Szczepanik, 2016). Considering the rapid growth of the AI technique, the application of AI can lead to innovation in nuclear engineering.

There have been several attempts to apply AI to specific designs in the field of nuclear engineering. The artificial neural network has been applied with supervised learning, which uses big data previously constructed in experiments or simulations for studies of reloading patterns in PWR cores (Filho et al., 2013; Montes and Ortiz, 2007; Ziver et al., 2002) or design of radiation shielding (Gencel, 2009). For applying artificial neural networks in the design of the reactor core, it has a limitation in obtaining big data from the particle transport simulations of a reactor core considering the high computation cost. Our previous studies investigating the feasibility of designs of the core pattern and fuel assembly (Kim et al., 2017b; Kim et al., 2018a, 2018b) using an artificial neural network revealed that the major problems in the application of AI for designing a research reactor core were (1) large

\* Corresponding author.

E-mail addresses: [songhyunkim@postech.ac.kr](mailto:songhyunkim@postech.ac.kr) (S.H. Kim), [shinsg@postech.ac.kr](mailto:shinsg@postech.ac.kr) (S.G. Shin), [sshan1214@postech.ac.kr](mailto:sshan1214@postech.ac.kr) (S. Han), [mhkim@postech.ac.kr](mailto:mhkim@postech.ac.kr) (M.H. Kim), [pyeon@rri.kyoto-u.ac.jp](mailto:pyeon@rri.kyoto-u.ac.jp) (C.H. Pyeon).

<https://doi.org/10.1016/j.pnucene.2019.103183>

Received 29 April 2019; Received in revised form 27 August 2019; Accepted 15 October 2019

0149-1970/© 2019 Elsevier Ltd. All rights reserved.

computational time for estimating reactor characteristics with the particle transport code and (2) many variables for the core design. These cause significant difficulty in the use of AI for designing the reactor core.

This study aims to investigate the feasibility of AI for automatic design of reactor cores for each reactor purpose. After construction of artificial neural networks for obtaining fluxes and multiplication factors in the core, a machine learning system of the artificial neural networks is constructed by developing an automatic MCNP simulation and analysis system. Also, a design procedure of the reactor core with AI is developed by imitating conventional design procedure. After setting a design goal with a simplified core of the Kyoto University Critical Assembly (KUCA), the core design is conducted using the design program developed in this study. After obtaining the assembly and core configurations, the performances are evaluated and verified by comparing them to cores designed by conventional design procedure.

## 2. Methods

### 2.1. Core and assembly configurations

The basic structure of the simplified KUCA core and the assembly are shown in Fig. 1 (Pyeon et al., 2015). The radial center of the core in Fig. 1 (a) is fixed to a void region without loading any assembly. Each fuel or reflector assembly can be loaded in the  $11 \times 11$  core except for the void region. In the fuel assembly, five kinds of plates (U10Mo (Fuel), graphite (Gr), beryllium (Be), polyethylene (PE) and lead (Pb)) surrounded by an Al-based sheath can be loaded in the fuel region as shown Fig. 1 (b) (Kim et al., 2017a, 2017b). The axial reflectors (or reflector assembly) can be axially arranged by sandwiching the fuel region, and four kinds of materials except for the U10Mo fuel can be loaded in the reflector regions. The maximum height of the fuel region is 49.8475 cm, and the length of each axial reflector is 500.0 mm. The size of the plate is  $5.08 \text{ cm} \times 5.08 \text{ cm} \times 0.3175 \text{ cm}$ , and 157 plates can be, therefore, axially loaded in the fuel region. Also, the four kinds of reflector assemblies surrounded by the Al-based sheath can be loaded in the core, as shown in Fig. 1 (c). The details of the material composition used in this study are given in Table 1.

For the feasibility study of the AI design applicability to the core design, a design goal was set to obtain the highest fast flux (defined as the neutron energy over 1 MeV) in the center of the core (a void region having specific volume without inserting any assembly as defined in Sec. 2.2) with a constant power. With the assumption of the constant power, the total number of neutrons generated by fission reactions in the core can be approximate to a constant. And, the highest fast flux in the void region having the fixed volume can be, therefore, obtained by Monte Carlo eigenvalue simulations even though the core configurations are changed. Also, it was set so that the goal multiplication factor of the core is  $1.015 \pm 0.005$ . In addition, the control rods used for controlling the criticality of the core were not considered in this study.

### 2.2. Method

The design goals given in Sec. 2.1 are to design an optimized reactor core with AI for obtaining maximum fast flux ( $E_n$  (neutron energy)  $> 1 \text{ MeV}$ ) while having a multiplication factor between 1.01 and 1.02. One solution to design the optimized core with AI is to conduct machine learning with random selections of all the materials for plates and assemblies. However, it is almost impossible to obtain big data with the large variables of the core: (1) the combinations of the fuel assembly are  $5^{157} \times 4^2$ , and (2) the combinations of the core with the fuel and reflector assemblies in 120 meshed regions are  $(5^{157} \times 4^2 + 4)^{120}$ .

In this study, the following design rules imitating conventional design procedure were used to reduce the variables:

- Two types of fuel assemblies are designed by AI: (1) the fuel assembly for obtaining the highest multiplication factor and (2) the fuel assembly for obtaining the highest fast flux with  $k_{eff} > 1.20$ .
- Fuel assemblies are axially symmetric, and the center of an assembly is fixed to the fuel plate.
- Unit cells as shown in Fig. 2 (a) containing 4 to 7 sub plates are repeatedly filled in the fuel region. Therefore, 38, 30, 26, and 22 cells are inserted in an assembly for the cases of a 4-Unit Cell, 5-Unit Cell, 6-Unit Cell, and 7-Unit Cell, respectively.
- The plates located over the top fuel plate and under the bottom fuel plate are replaced with reflector material, as shown in Fig. 2 (b).
- For the design of the fuel assembly, the reflective and vacuum boundary conditions are used as shown in Fig. 1 (b).
- Flux tally is conducted in the fuel region, and the energy boundaries of the flux tally are set to 0 eV, 1 MeV, and 100 MeV.

#### (b) Core

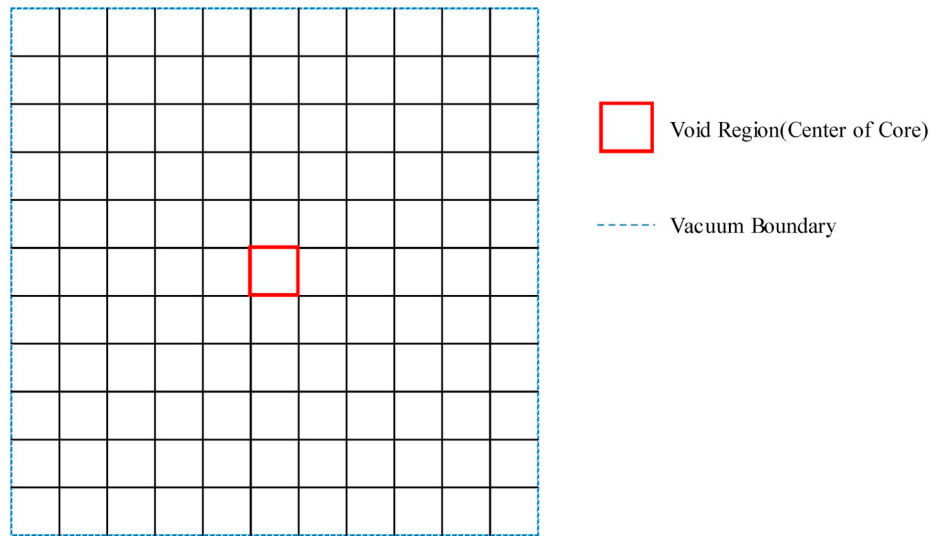
- The 1/8 core is assumed and no assembly can be loaded in the center region shown in Fig. 3 (a).
- The vacuum boundary conditions are used as shown in Fig. 1.
- The fuel assemblies cannot be loaded in the reflector assembly region, as shown in Fig. 3.
- Fluxes are scored in a hexahedral tally region ( $5.08 \text{ cm} \times 5.08 \text{ cm} \times 6.0325 \text{ cm}$ ) located at the center of the void region (Fig. 3 (b)), and the energy boundaries of the tally are set to 0 eV, 1 eV, 1 MeV, and 100 MeV.
- The goal for the effective multiplication factor of the core is 1.01.

Based on the design rules, the designs of fuel assemblies and core were conducted with the AI design algorithm proposed in this study. The overview of the algorithm is shown in Fig. 4. To minimize the possible cases for the core design, the fuel assemblies are first designed, and the design of the core with the reflector assemblies is conducted with the designed fuel assemblies. In the design algorithm, each artificial neural network with the sigmoid activation function was trained by the gradient descent optimizer and learning rate adaptation method (Jacobs, 1988).

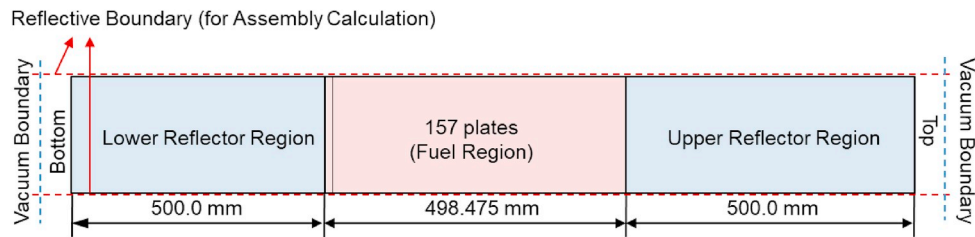
For designing the fuel assemblies, a combination of the plates in each unit cell given in Fig. 2(a) is chosen for obtaining the highest multiplication factor. Another combination of the plates in each unit cell is chosen for obtaining the highest fast flux per total flux having  $k_{eff} > 1.2$ . With the two design goals, designs of the fuel assemblies with the artificial neural network are individually conducted with the following steps:

- (1) Using the assembly models shown in Fig. 2 and 50 random cases (the combinations of the plates) are sampled for all the four unit-cell assemblies with random sampling of the unit cells. An optimized flag #1, which is used for deducing the optimized design of the fuel assemblies, is set to 0.
- (2) The MCNP6.1 code simulations with the cases generated in Step 1 are conducted with the ENDF VII.0 cross-section library (Pelowitz, 2013). In the MCNP calculations, 1,000 histories per cycle, 10 skip cycles, and 120 active cycles were used for efficiently obtaining the big data. In this calculation, the convergence of fission-source distributions is checked by the Shannon entropy method (Ueki and Brown, 2002), and the skip cycle is doubled when the fission source distribution does not converge.
- (3) The multiplication factor and fluxes are extracted from the outputs of the MCNP simulations. The multiplication factor is divided by 2.0 (maximum multiplication factor expected for the assembly design) to obtain outputs between 0.0 and 1.0 as using the sigmoid activation function in the artificial neural network,

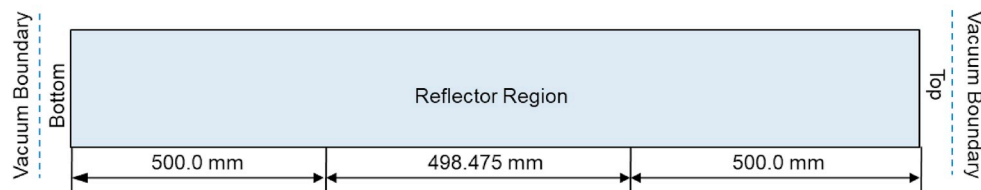
#### (a) Fuel assembly



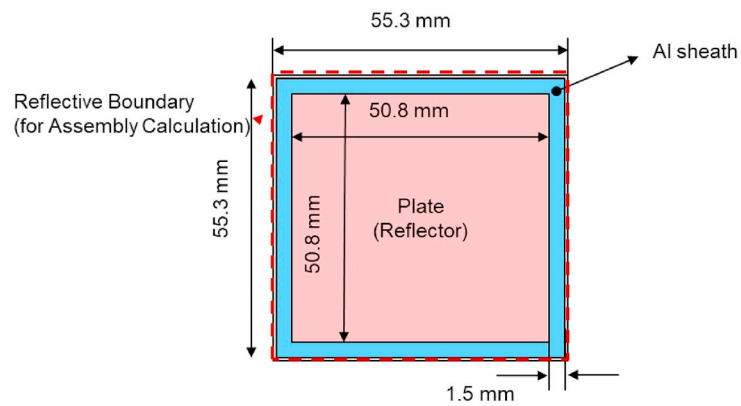
(a) Radial View of 11 x 11 Core



(b) Axial View of Fuel Assembly



(c) Axial View of Reflector Assembly



(d) Radial View of Assembly

Fig. 1. Conceptual overview of the simplified KUCA core.

**Table 1**

Details of material compositions for plates used in this study.

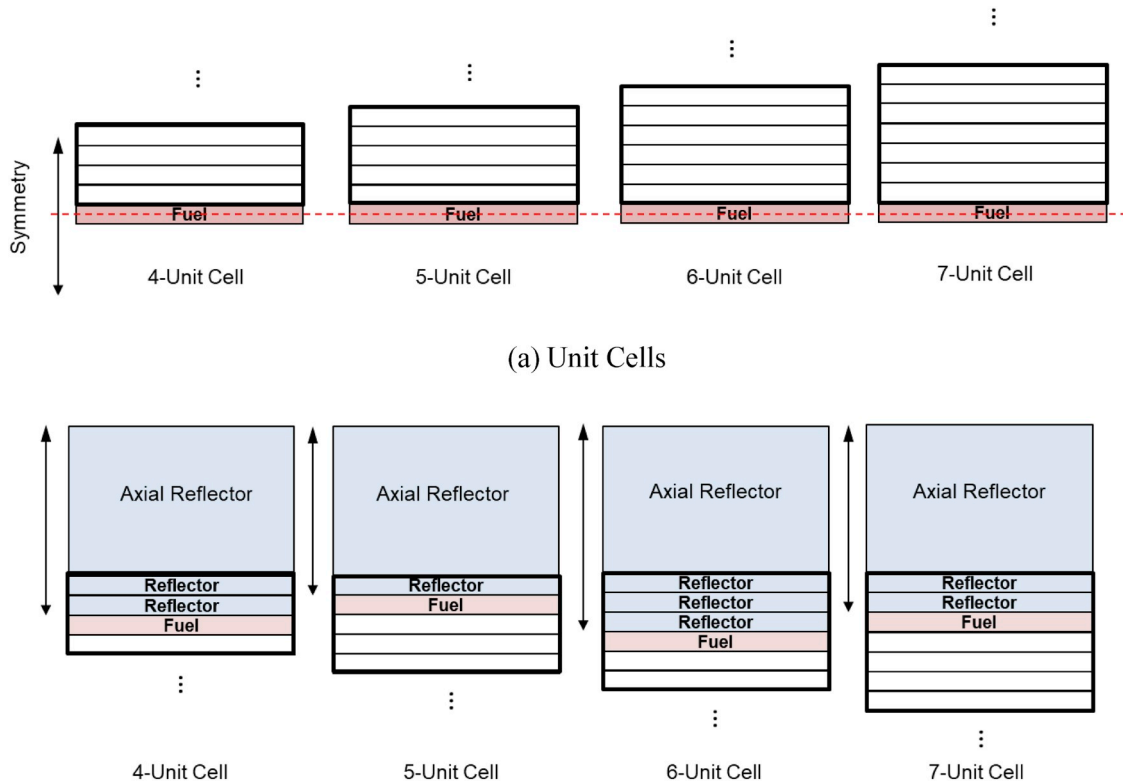
Material Type	Nuclide	Atomic number density [ $\times 10^{24}/\text{cm}^3$ ]
Fuel: U10Mo LEU (Homogenized by Al cladding)	Mo-92	8.3664E-04
	Mo-94	5.3283E-04
	Mo-95	9.2680E-04
	Mo-96	9.8126E-04
	Mo-97	5.6767E-04
	Mo-98	1.4491E-03
	Mo-100	5.9013E-04
	U-234	5.6445E-05
	U-235	4.2694E-03
	U-236	9.9017E-05
	U-238	1.6975E-02
	Al-27	2.7070E-02
	B-10	2.6889E-07
	B-11	1.0823E-06
	82204	4.66819E-04
	82206	8.03596E-03
Pb	82207	7.36908E-03
	82208	1.74724E-02
Gr	6000	8.64182E-02
PE	1001	7.77938E-02
	6000	3.95860E-02
Al	13027	6.00385E-02
Be	4009	8.64182E-02

and the fast flux ( $\#/\text{cm}^2$ ) over 1 MeV is divided by total flux at each simulation. The results are updated in the big data to perform the machine learning.

- (4) While constructing two neural networks for individually obtaining the multiplication factor and the fast to total flux ratio, the machine learning of the feedforward neural networks used for design of the fuel assembly is conducted using the back-propagation algorithm (Bryson and Ho, 1969). In each neural network, three layers including the input of the neural network

(Kim et al., 2017b) are adopted. The numbers of neurons in the input, hidden, and output layers are 400, 80 and 1, respectively. The number of regions in the assembly model are 80 (half of the assembly); 5 types of materials can be inserted in each region. As selecting a material in a region, one of the five input neurons linked to the region is activated to 1 while the other input neurons linked to the region are inactivated to 0.

- (5) Using the neural networks, two types of fuel assemblies, which have different goals in the assembly design, are designed. In the designs made by the artificial neural network, the initial plates are assumed to be the fuel plates, and the plate and the reflector are individually replaced by other materials for obtaining the design goals.
- (6) After designing the fuel assemblies, two fuel assemblies (the fuel assembly for obtaining the highest multiplication factor, and the fuel assembly for obtaining the highest fast flux ratio with  $k_{eff} > 1.20$ ) optimized by the artificial neural networks are produced for each unit cell. The optimized designs are stored and compared with the assembly designed in the previous iteration step. If the optimized designs are equal to those of the previous step, Step 8 is conducted; otherwise, Step 7 is conducted.
- (7) With the eight assembly designs (based on the four unit-cells for the multiplication factor and the neutron flux), five cases for each design are generated. The first case is the design generated by the neural network for obtaining the best result with the design goal. Then four (or nine if the optimized flag #1 = 1) cases are generated by the genetic algorithm that is the crossover and mutation techniques. The cross over technique is conducted by exchanging two plates randomly selected in a unit cell. For the mutation technique, two plates in a unit cell are randomly sampled, and the materials of the plates are randomly changed to the other materials. In addition, the axial reflector is randomly changed. Based on the design rules of the fuel assembly, MCNP input is generated, and Step 2 calculations are conducted.

**Fig. 2.** Definitions of unit cells and reflector loading strategy.

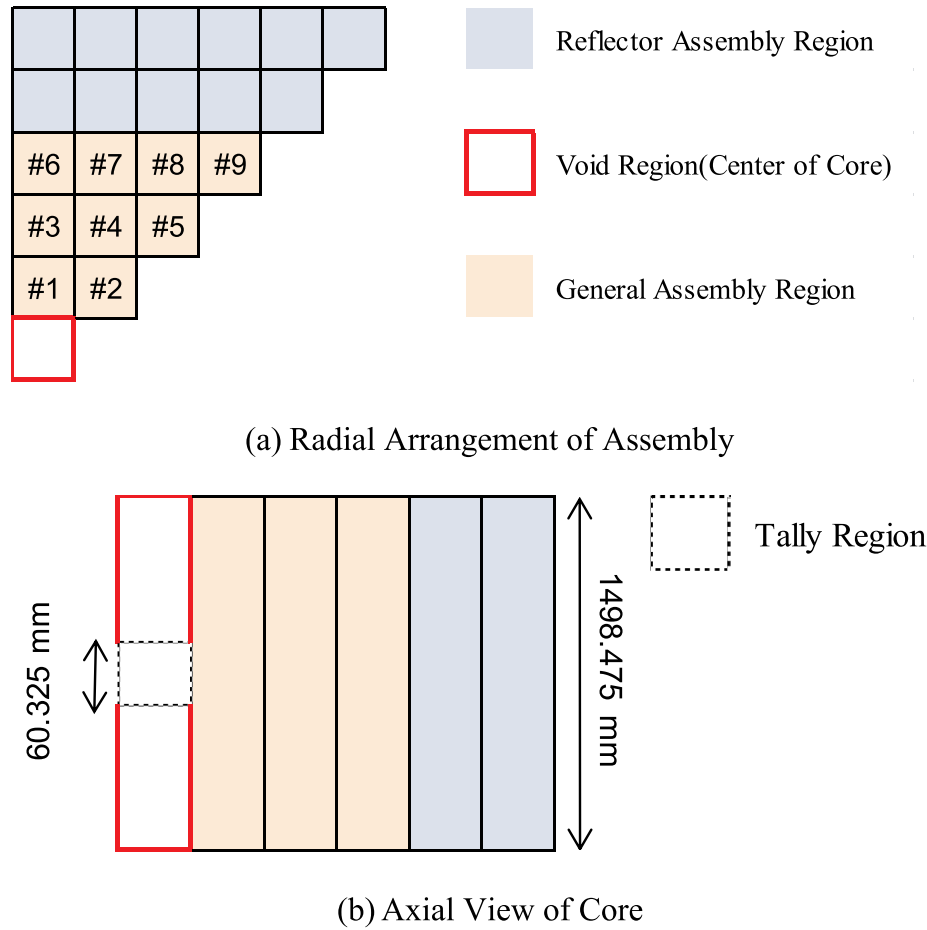


Fig. 3. Overview of core design scheme in this study.

- (8) If the optimized flag #1 is 0, flag #1 is changed to 1, and go to Step 7. If the optimized flag #1 is 1, the iteration for designing the fuel assembly is stopped, and the assemblies are selected.

For designing the core, the designs of the fuel assemblies optimized in previous steps (Steps 1–8), are used. The details of the design algorithm for the KUCA core are given as follows.

- (9) From the fuel assemblies obtained in Steps 1–8, three unit cells showing higher performances for the multiplication factor and the neutron flux are selected, respectively. If the combination of plates is equal among the different unit cells, one of the unit cells is selected. It is assumed that the five active heights of each fuel assembly are used by considering the size of the unit cell as shown in Table 2. With the fuel assemblies, the reflector assemblies based on the Gr, Be, PE, and Pb blocks are used in the core design.
- (10) Using the fuel (Fig. 5) and reflector assemblies with the core model (Figs. 3), 50 cases produced by inserting the fuel and reflector assemblies are randomly sampled.
- (11) The MCNP6.1 code simulations with the sampled cases (core) are conducted with the ENDF VII.0 cross-section library. In the MCNP calculations, 2,000 histories per cycle, 20 skip cycles, and 100 active cycles were used.
- (12) The multiplication factor and fluxes at the tally region (Fig. 3 (b)) are extracted from the outputs. The multiplication factor is divided by 2.0 (maximum multiplication factor expected for the core design) to obtain outputs between 0.0 and 1.0 as using the sigmoid activation function in the artificial neural network, and the fast flux ( $\#/\text{cm}^2$ ) over 1 MeV and the thermal flux under 1 eV

are directly used. The outputs with the input for obtaining the results are updated in the big data to perform the machine learning.

- (13) The machine learning of the A, B, and C feedforward neural networks as shown in Fig. 4 are conducted for obtaining the effective multiplication factor, thermal flux, and fast flux, respectively. In each neural network, three layers including the input of the neural network are adopted (Kim et al., 2017b), and the numbers of neurons in the input, hidden, and output layers are 504, 21, and 1, respectively. The number of regions in the core model are 21; four types of fuel assemblies having five different active heights (Table 2) and four types of reflector assemblies can be inserted in each region. Therefore, the number of input neurons linked to each region is 24. As selecting an assembly in a region, one of the 24 neurons linked to the region is activated to 1 while the other neurons linked to the region are inactivated to 0.
- (14) Core design is conducted using the artificial neural networks after the machine learning. First, all meshed regions are initialized to the Be reflector assemblies. Then the following design procedures are used for obtaining an optimized core design:
- The fuel assemblies in the #1 and #2 meshed regions, which are adjacent to the void region (Fig. 3 (a)), are first chosen to obtain the highest fraction of the fast to thermal fluxes estimated by the B and C artificial neural networks;
  - The fuel or reflector assemblies are loaded in order of the number of the meshed region from #3 until it reaches the goal effective multiplication factor 1.02;



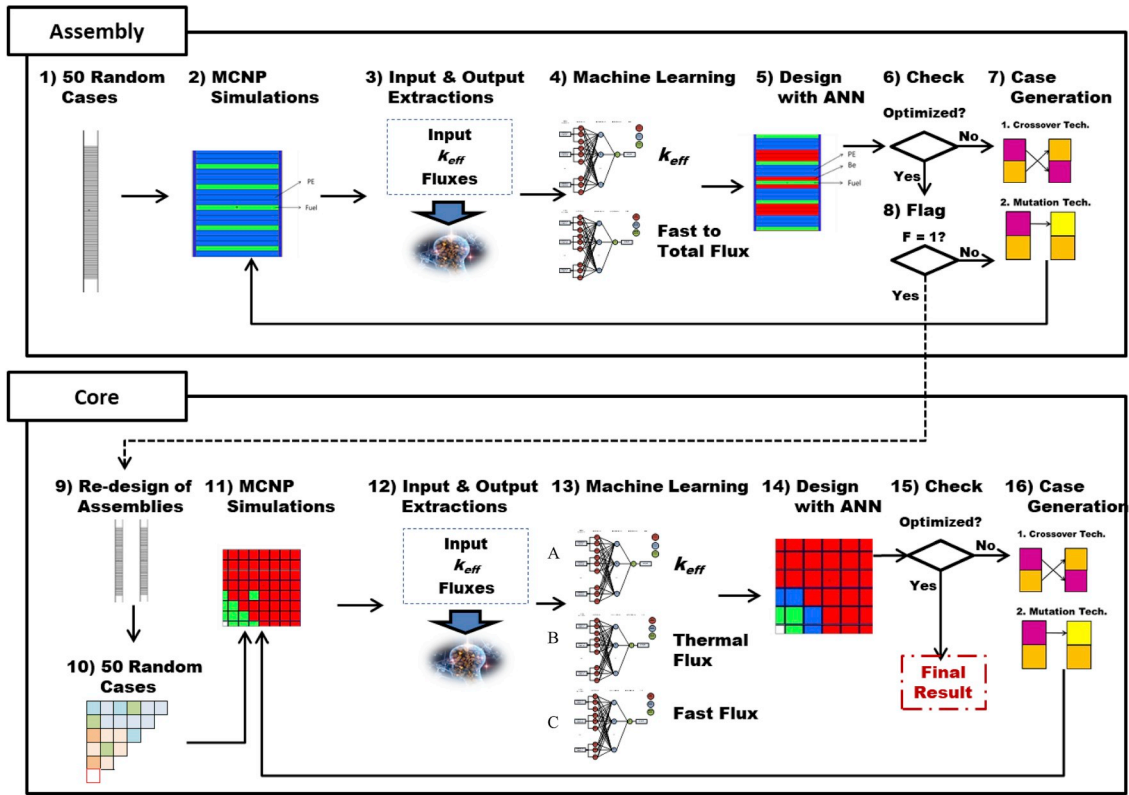


Fig. 4. Design strategy of the assemblies and core proposed in this study.

**Table 2**  
Active heights for the fuel assemblies used in the core design.

Type of Fuel Assembly	Number	Active Height [cm]
Fuel Only	1	49.8475
	2	43.4975
	3	37.1475
	4	30.7975
	5	24.4475
5-Unit Cell	1	47.9425
	2	41.5925
	3	35.2425
	4	28.8925
	5	22.5425
6-Unit Cell	1	49.2125
	2	41.5925
	3	33.9725
	4	26.3525
	5	18.7325
7-Unit Cell	1	47.9425
	2	43.4975
	3	39.0525
	4	34.6075
	5	30.1625

generated by the mutation technique. In using the mutation technique, the random change probability of the assembly type is 0.3, and only the same type of assembly (fuel and reflector) is allowed. After generating the 20 cases, Step 11 is conducted.

### 3. Result and analysis

Automatic design programs (ADP) based on the methods given in Sec. 2.2 were developed with the C++ program language. The total computation times for the assembly and core designs including the machine learning process were about 18.6 (total number of data accumulated = 1,130 #) and 50.6 h (total number of data accumulated = 2,370 #) with a single core processor, respectively. After obtaining the optimized assemblies and core designed by ADP, the MCNP6 simulations were conducted to verify the core designed by the proposed method. In the calculations, 5,000 histories per cycle, 20 skip cycles, and 220 active cycles were used with ENDF VII.0 cross section library.

The fuel assemblies designed by ADP are shown in Fig. 5, and the effective multiplication factor and the neutron fluxes scored in the fuel region for the fuel assemblies are given in Table 3. The plate combinations of the fuel assemblies showing the highest fast to thermal flux satisfying  $k_{eff} > 1.2$  were chosen to insert all fuel plates in the fuel region for all unit cells, as shown in Fig. 5 (a), which is the same assembly configuration as that designed in the previous study (Kim et al., 2017a, 2017b). The fuel assemblies for obtaining “highest effective multiplication factor” with the unit cells were designed as shown in Fig. 5 (b)–(e); as the reflector, BE for all unit cells was chosen by ADP. The effective multiplication factors with the fuel assemblies designed by ADP showed high values while using fewer fuel plates than were used by the fuel assemblies designed in the previous studies (Pyeon et al., 2012, 2016). Especially, the fuel assembly with the unit cell containing seven sub plates gave the highest effective multiplication factor even though it has the fewest fuel plates.

From the results in above, the four fuel assemblies (5-Unit Cell, 6-

- iii. The reflector assemblies are chosen to obtain the highest effective multiplication factor;
- iv. From the meshed regions #1 to #9, each assembly is re-decided for obtaining the highest fast flux at the void region (Tally Region in Fig. 3 (b)) while maintaining the effective multiplication factor between 1.01 and 1.02.
- (15) The current core design is compared to the core design optimized in the previous iteration step. If the design is equal to the previous design, the core design is adopted; otherwise, Step 16 is conducted.
- (16) For the machine learning, 20 cases are additionally generated. One is the designed core conducted in Step 15, and others are

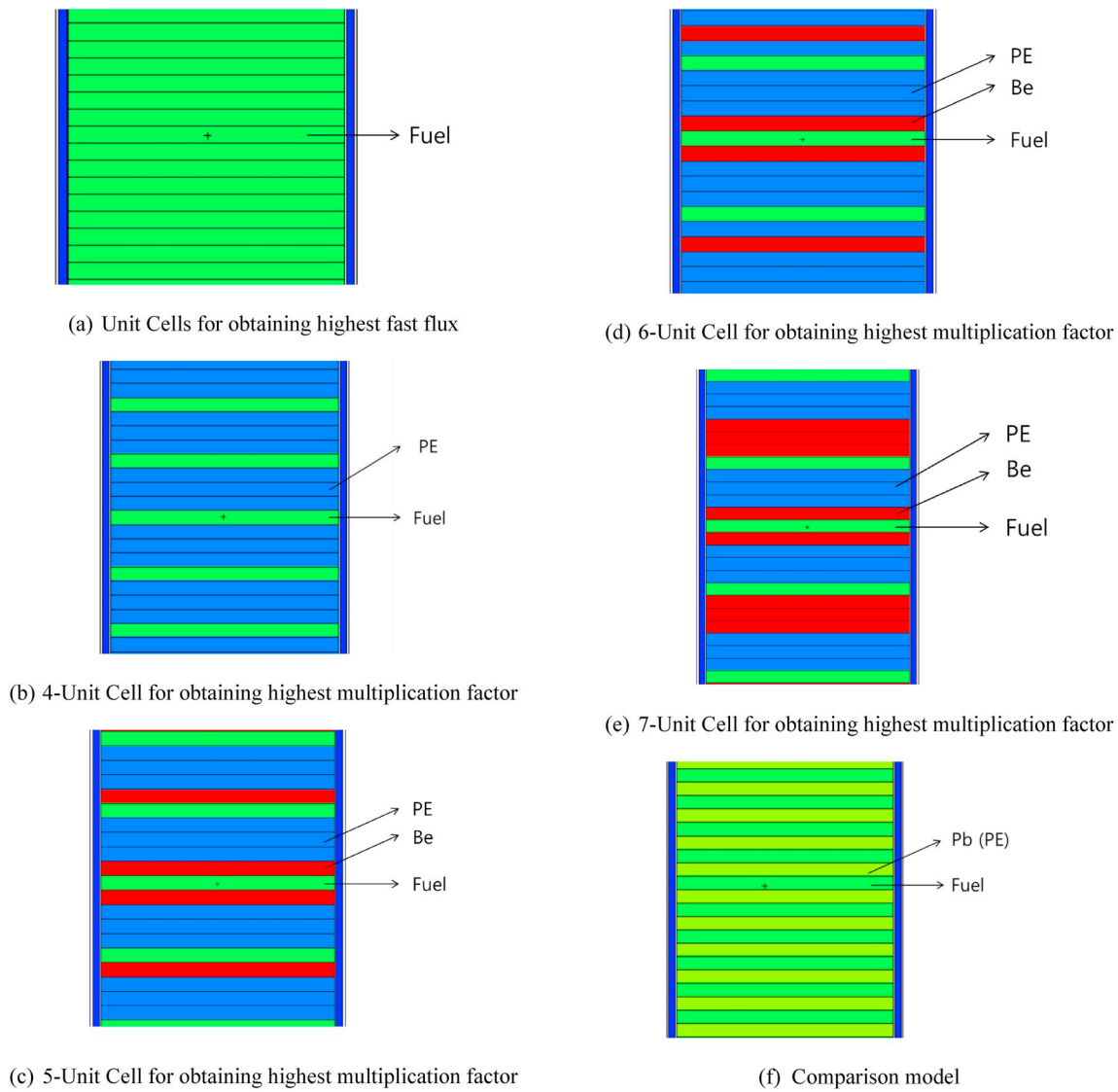


Fig. 5. Design results and comparison models for fuel assembly.

Table 3

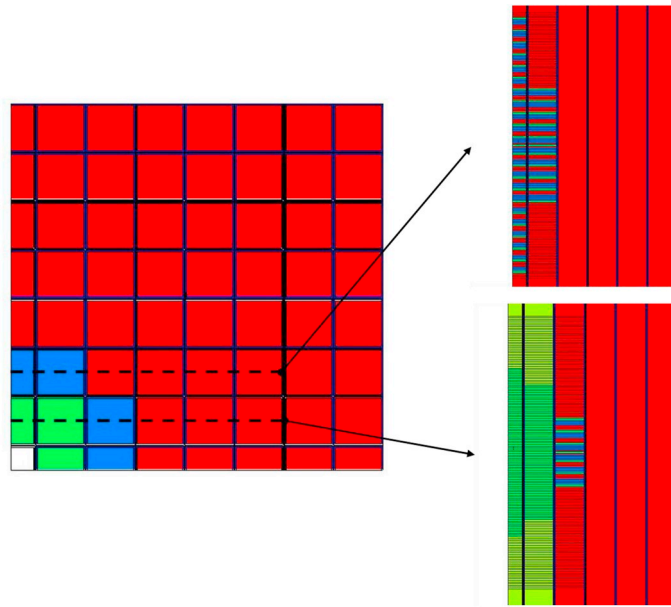
Effective multiplication factors and fluxes for the fuel assemblies.

Fuel Type	Reflector	# of Fuel Plates	$k_{eff}$	Fast to Total Flux	Thermal to Total Flux
Fuel Only	Pb	157	1.32340 ( $\pm 0.00055$ )	69.90%	0.00%
4-Unit Cell	Be	39	1.62879 ( $\pm 0.00064$ )	49.22%	25.23%
5-Unit Cell	Be	31	1.64427 ( $\pm 0.00062$ )	47.18%	26.51%
6-Unit Cell	Be	27	1.64989 ( $\pm 0.00057$ )	45.01%	30.41%
7-Unit Cell	Be	23	1.65419 ( $\pm 0.00072$ )	44.06%	28.62%
Pb – Fuel <sup>a</sup>	Pb	79	1.15230 ( $\pm 0.00047$ )	65.65%	0.00%
PE – Fuel <sup>a</sup>	PE	79	1.39664 ( $\pm 0.00069$ )	56.78%	13.36%

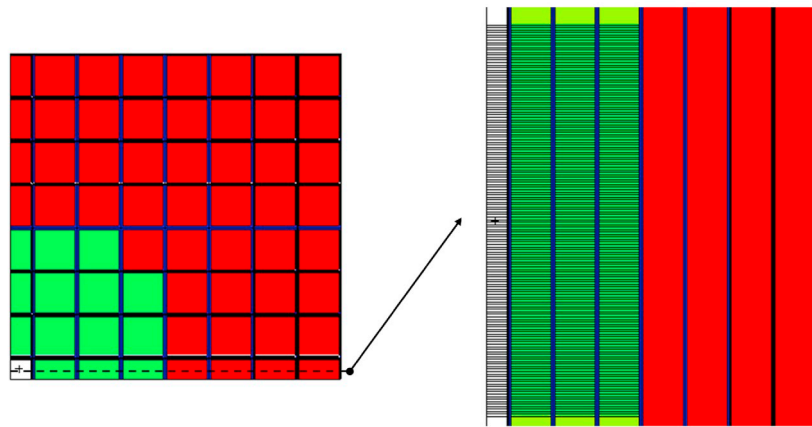
<sup>a</sup> The fuel and Pb (PE) plate is filled in the fuel region in order, as shown in Fig. 5 (f).

Unit Cell, 7-Unit Cell, and Fuel Only selected by Step 9) were selected for the core design. Using ADP with the fuel assemblies and the moderator assemblies, the core was designed as shown in Fig. 6 (a). For the verification, two cases of the cores having  $k_{eff} \sim 1.01$  were additionally designed considering previous studies (Kim et al., 2017a,2017b; Pyeon et al., 2016), as shown in Fig. 6 (b) and (c). In Case #1 (Fig. 6 (b)), fuel plates were filled only in the fuel region without moderator; Pb is used as the axial reflector. Also, the Be block is used as the radial reflector. In Case #2 (Fig. 6 (c)), the assembly with the Pb-fuel combination filled in the fuel region was used near the void region with the Pb axial reflector

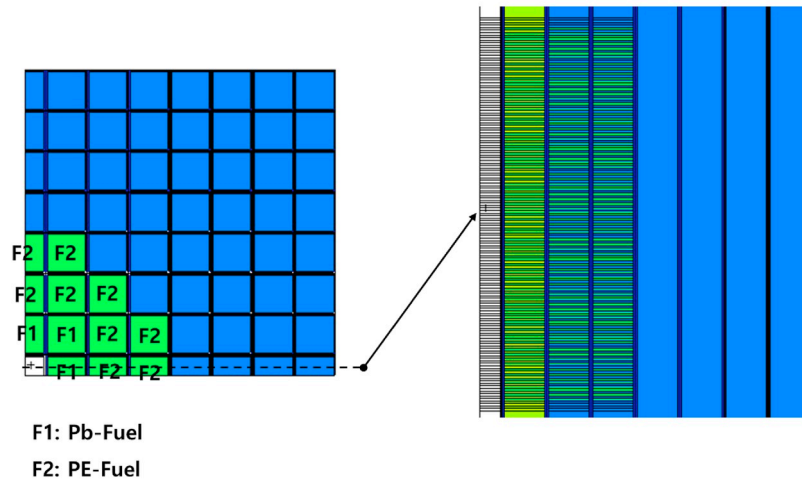
to increase the fast flux. Also, the PE-fuel combination was used in the other fuel region with the PE axial and radial reflectors to increase the effective multiplication factor. The effective multiplication factors and fluxes with the core conditions were estimated as shown in Table 4. The design goal of the core was “obtaining the highest fast flux in the tally region”, and the fast flux of the core designed by ADP was 178% and 301% higher than those of the cores designed by the conventional design procedure. The core designed by ADP was semi-spherically arranged, and the fuel assemblies near the target region have many fuel plates, whereas the fuel assemblies containing moderator plates have few fuel



(a) Core designed by proposed method



(b) Comparison Case #1



(c) Comparison Case #2

Fig. 6. Core design with the proposed method and additional cases.



**Table 4**  
Effective multiplication factors and fluxes for the simplified KUCA core.

Core Type	Active Height	$k_{eff}$	Fast Flux <sup>a</sup> (>1 MeV)	Thermal Flux <sup>a</sup> (<1eV)	Total Flux <sup>a</sup>
Core Designed by ADP	–	1.00924 (±0.00081)	1.02E-04	3.54E-06	1.35E-04
Case #1	49.8475 cm	1.01280 (±0.00067)	5.71E-05	1.04E-07	7.46E-05
Case #2	47.3075 cm	1.01031 (±0.00083)	3.38E-05	1.38E-06	4.59E-05

<sup>a</sup> Unit: #/cm<sup>2</sup>-source.

plates. This specific configuration of the core led to the high fission reactions near the tally region with absorbing the thermal neutrons.

#### 4. Conclusions

A feasibility study of the design optimization of reactor core using artificial neural network was conducted. For verifying the design feasibility, a simplified KUCA model was selected, and a specific goal for the core design with the artificial intelligence was set to obtain the highest fast flux at the same reactor power. The design method of the fuel assemblies and core using the artificial neural network was proposed with imitating the conventional design procedures. After developing the automatic design program based on the artificial neural network, the core was designed and compared with those designed with the assemblies used in previous studies. The total computation times for the assembly and core designs including the machine learning were 18.6 and 50.6 h with a single core processor, respectively. The computation costs were achieved by using 1) various assumptions imitating the conventional design procedure, 2) the small particle history in Monte Carlo simulations, and 3) the machine learning algorithm with generating important data based on the target outputs. The design goal (for obtaining high fast flux) of the core designed by the proposed method was incredibly achieved compared to those designed by the conventional design procedure. It is expected the application of the artificial intelligence to reactor designs can lead to innovations as well as achieve high performances on specific purposes of reactor cores.

#### Acknowledgements

This work was supported by a National Research Foundation of Korea (NRF) grant funded by the Ministry of Science and ICT of Korea (MSIT) (NRF-2018M2C7A1A02071506).

#### Appendix A. Supplementary data

Supplementary data to this article can be found online at <https://doi.org/10.1016/j.pnucene.2019.103183>.

#### References

- Bryson, A.E., Ho, Y.C., 1969. Applied Optical Control: Optimization, Estimation, and Control. Blaisdell, New York, ISBN 0-89116-228-3.
- Filho, L.P., Souto, K.C., Machado, M.D., 2013. Using neural networks for prediction of nuclear parameter. In: 2013 International Nuclear Atlantic Conference (INAC 2013), PE, Brazil, November 24–29; 2013.
- Gencel, O., 2009. The application of artificial neural networks technique to estimate mass attenuation coefficient of shielding barrier. Int. J. Phys. Sci. 4, 743–751.
- Jacobs, R.A., 1988. Increased rates of convergence through learning rate adaptation. Neural Netw. 1 (1988), 295–307.
- Kim, S.H., et al., 2017. A feasibility study on fast reactor with low-enriched uranium fuel at kyoto university critical assembly. Prog. Nucl. Energy 100 (2017), 1234–1239.
- Kim, S.H., et al., 2017. A preliminary study on applicability of artificial neural network for optimized reflector designs. Energy Procedia 131 (2017), 77–85.
- Kim, S.H., et al., 2018. Kinetics solution with iteration scheme of history-based neutron source in accelerator driven system. Ann. Nucl. Energy 112 (2018), 337–353.
- Kim, S.H., et al., 2018. Design of LEU fuel assembly using artificial neural network at kyoto university critical assembly. In: Transactions of the Korean Nuclear Society Spring Meeting Jeju, Korea, (May 2018 (2).
- LeCun, Y., Bengio, Y., Hinton, G., 2015. Deep learning. Nature 521 (2015), 436–444.
- Montes, J.L., Ortiz, J.J., 2007. LPPF prediction in a BWR fuel lattice using artificial neural network. In: Joint International Topical Meeting on Mathematics & Computation and Supercomputing in Nuclear Application (M&C + SNA 2007), Monterey, California, April 15–19; 2007.
- Nozaki, N., et al., 2017. Application of artificial intelligence technology in product design. Fujitsu Sci. Tech. J. 53 (2017), 43–51.
- Pelowitz, D.B., 2013. MCNP6™ User Manual Version 1.0, LA-CP-13-00634. Los Alamos National Laboratory.
- Persson, C.M., et al., 2008. Pulsed neutron source measurements in the subcritical ADS experiment YALINA-booster. Ann. Nucl. Energy 35 (2008), 2357–2364.
- Poteralski, A., Szczepanik, M., 2016. The application of artificial intelligence in the optimal design of mechanical systems, 2016. IOP Conf. Ser. Mater. Sci. Eng. 161 (2016), 012040.
- Pyeon, C.H., et al., 2009. First injection of spallation neutrons generated by high-energy protons into the kyoto university critical assembly. J. Nucl. Sci. Technol. 46 (2009), 1091–1093.
- Pyeon, C.H., et al., 2012. Accuracy of reaction rates in the accelerator-driven system with 14 MeV neutrons at the Kyoto University Critical Assembly. Ann. Nucl. Energy 40 (2012), 229–236.
- Pyeon, C.H., et al., 2015. Neutron characteristics of solid targets in accelerator-driven system with 100-MeV protons at kyoto university criticality assembly. Nucl. Technol. 192 (2015), 181–190.
- Pyeon, C.H., et al., 2016. Validation of Pb nuclear data by Monte Carlo analyses of sample reactivity experiments at Kyoto University Critical Assembly. J. Nucl. Sci. Technol. 53 (2016), 602–612.
- Ueki, T., Brown, F.B., 2002. Stationarity diagnostics using Shannon entropy in Monte Carlo criticality calculation I: F test, trans. Am. Nucl. Soc. 87, 156.
- Yamanaka, M., et al., 2016. Accuracy of reactor physics parameters in torium-loaded accelerator driven system experiments at kyoto university critical assembly. Nucl. Sci. Eng. 183 (2016), 96–106.
- Ziver, A.K., et al., 2002. On the Use of Artificial Neural Network in Loading Pattern Optimization of Advanced Gas-Cooled Reactors, vol. 2002. PHYSOR, Seoul, Korea. October 7–10; 2002.